arXiv:astro-ph/0202043v2 3 Sep 2002

Limits to the Cas A ^{44}Ti Line Flux and Constraints on the Ejecta Energy and the Compact Source

R. E. Rothschild & R. E. Lingenfelter

Center for Astrophysics and Space Sciences, 0424,
University of California at San Diego, 9500 Gilman Dr., La Jolla, CA 92093

rrothschild@ucsd.edu & rlingenfelter@ucsd.edu

ABSTRACT

Two long observations of Cas A supernova remnant were made by the *Rossi X-ray Timing Explorer* in 1996 and 1997 to search for hard X-ray line emission at 67.9 and 78.4 keV from the decay of ^{44}Ti formed during the supernova event. Continuum flux was detected up to 100 keV, but the ^{44}Ti lines were not detected. The 90% confidence upper limit to the line flux is 3.6×10^{-5} photons cm^{-2}s^{-1}. This is consistent with the recent *BeppoSAX* detection and with the *CGRO*/COMPTEL detection of the companion transition line flux for ^{44}Sc decay. The mean *BeppoSAX*—COMPTEL flux indicates that $1.5\pm0.3\ \times10^{-4}$M$_{\odot}$ of ^{44}Ti was produced in the supernova explosion. Based upon recent theoretical calculations, and optical observations suggesting a WN Wolf-Rayet progenitor with an initial mass of $\geq$25 M$_{\odot}$, the observed ^{44}Ti yield implies that the Cas A supernova ejecta energy was $\sim2\times10^{51}$ ergs, and as a result a neutron star was formed, rather than a black hole. We suggest Cas A is possibly in the early stages of the AXP/SGR scenario in which the push-back disk has yet to form, and when the disk does form, the accretion will increase the luminosity to that of present-day AXP/SGRs and pulsed emission will commence.

Subject headings: nuclear reactions, nucleosynthesis, abundances — supernova remnants — X-rays: individual (Cassiopeia A)

1. Introduction

Optical observations suggest that Cas A is the remnant of a Type Ib/c supernova whose progenitor was a WN Wolf-Rayet star with initial mass greater than 25 M$_{\odot}$ (Fesen 2001; Fesen & Becker 1991; Jansen et al. 1988). The discovery of a point source at the center of the remnant by *Chandra* (Tananbaum 1999) is strongly indicative of the creation of a neutron star or black hole in the event, and would be consistent with such a progenitor. Subsequent observations by *Chandra* (Chakrabarty et al. 2001; Murray et al. 2001) and *XMM* (Mereghetti, Tiengo, & Israel 2001) have confirmed the point source nature of the object, but the existence of pulsations (and therefore a neutron star) is still questionable. Comparison of supernova explosion models (Woosley & Weaver 1995; Nakamura et al. 2001) with measurements of the amount of ^{44}Ti created, can be used to estimate the remnant core mass and, therefore, the nature of the compact object.

^{44}Ti is produced by explosive Si burning and the freeze out from nuclear statistical equilibrium in supernovae, and is believed to be the primary source of ^{44}Ca (Timmes et al. 1996). ^{44}Ti decays with a

59.2 ± 0.6 year half-life (Ahmad et al. 1998; Görres et al. 1998; Norman et al. 1998) to ^{44}Sc producing two nuclear lines at 67.9 and 78.4 keV of essentially equal intensity. The ^{44}Sc decays to the first excited state of ^{44}Ca which then emits a gamma-ray of 1157 keV with a 3.93 hour half-life to reach the ground state. All three nuclear lines are expected to have essentially the same line strength. Given the half-life of ^{44}Ti, the distance to Cas A (3.4 kpc; Reed et al. (1995)), the time since the supernova (317 yr for a mean observation date of 1997; Ashworth (1980)), and the observed line flux, one can estimate the amount of ^{44}Ti created.

Attempts to detect the ^{44}Ti lines began with the analysis of galactic scanning observations by the germanium spectrometer on *HEAO-3* (Mahoney et al. 1992). A 1σ limit of 8.3×10^{-5}photons cm^{-2}s^{-1} from a point source anywhere in the galaxy was determined for the ^{44}Ti line flux. Initial results from *CGRO*/COMPTEL observations of Cas A announced the discovery of 1.157 MeV line flux from the ^{44}Sc decay (Iyudin et al. 1994), and this was revised after further observations to be $3.3\pm0.6\times10^{-5}$photons cm^{-2}s^{-1} (Iyudin 1999). *CGRO*/OSSE observations of Cas A provided for a simultaneous fit to the three nuclear lines, and yielded a 99% confidence upper limit of 5.1×10^{-5}photons cm^{-2}s^{-1} (The et al. 1995), with detection of the continuum radiation to 40 keV (The et al. 1996). With the launches of *RXTE* and *BeppoSAX* in 1995 and 1996, two powerful hard X-ray instruments became available for ^{44}Ti line searches. The initial *RXTE*/HEXTE result was a 2.4σ detection ($4.3\pm1.8\times10^{-5}$photons cm^{-2}s^{-1}) during one long observation and no detection ($-1.4\pm1.7\times10^{-5}$ photons cm^{-2}s^{-1}) in another (Rothschild et al. 1998a). Similarly, initial *BeppoSAX*/PDS measurements could only claim an upper limit ($\leq5\times10^{-5}$photons cm^{-2}s^{-1}; Vink (1998)). After additional observations, Vink et al. (2001) were finally able to claim a good detection with a flux of $2.1\pm0.7\times10^{-5}$photons cm^{-2}s^{-1} for the 68 and 78 keV lines from ^{44}Ti. In this article we present a reanalysis of the *RXTE*/HEXTE observations of Cas A that were begun before the Vink et al. (2001) announcement of the detection.

The $>$10 keV continuum upon which the ^{44}Ti lines lie has been fit historically to a power law with photon index $\sim$3 or a thermal bremsstrahlung model whose temperature is dependent upon the extent of the high energy limit to the data. Allen et al. (1997) used *ASCA*, *RXTE*, and *CGRO* data to show that the thermal models successful below 10 keV (2 Raymond-Smith components and a 6.4 keV Gaussian) fall well below the data above 10 keV. The addition of a broken power law ($\Gamma=1.8^{+0.5}_{-0.6}$ below $15.9^{+0.3}_{-0.4}$ keV and $\Gamma=3.04^{+0.15}_{-0.13}$ above) best described the data to 120 keV. Several authors (Laming 2001; Atoyan et al. 2000; Baring et al. 1999; Gaisser, Protheroe & Stanev 1998) have described the processes that may be involved in the photon continuum production in supernova remnants such as Cas A. A non-thermal bremsstrahlung component may become the dominant contributor at $\sim$100 keV, and therefore, its presence may affect the inferred photon flux from the ^{44}Ti lines for observations with high sensitivity above the line complex.

2. Observations

RXTE observed Cas A several times for calibration purposes (ObsIds 00022, 10418, 30804, and 40806) and twice as part of an investigation into the ^{44}Ti emission lines (ObsIds 10271 and 20253). The broad-band (2-60 keV) spectral results have been published by Allen et al. (1997), and this analysis concentrates on the 15-240 keV data from the High Energy X-ray Timing Experiment (HEXTE; Rothschild et al. (1998b)). The HEXTE is a set of eight NaI(Tl)/CsI(Na) scintillation detectors grouped into two clusters of four detectors each. The HEXTE detectors are mechanically collimated to a 1° FWHM field of view, and cover the 15-250 keV range. The full collecting area for HEXTE is 1400

cm^2 (spectral capability was lost from one HEXTE detector early in the mission).

The observation dates and accumulated livetimes are given in Table 1. Since the livetime associated with the calibration observations is quite small compared to that of the two long observations, the analysis presented here will be restricted to the latter set of data.

3. Data Reduction and Analysis

The HEXTE data were accumulated for each cluster using a script developed at UCSD and the University of Tübingen. The cluster data were separated into on-source, off-source-plus and off-source-minus, since each HEXTE cluster collects real-time background data from two independent positions $\pm 1.5^\circ$ to either side of the on-source position. The two clusters' rotation axes are orthogonal to each other, and in this way four independent background regions are sampled. By comparing the two off-source positions for a given cluster, one can determine if a confusing source is contaminating one of the background regions, and if so, eliminate it from further analysis. The background observations are 75% as long as the on-source observations, since the time to move the pointing position on- and off-source comes out of the background observations. This ensures HEXTE continual on-source coverage.

The two background histograms from each cluster were tested for a confusing source by specifying the off-minus data as the source and the off-plus data as the background in the HEASARC spectral fitting program XSPEC (Arnaud 1996). The net count rate was compared to the ideal value of 0.0, and the spectra were examined for a continuous deviation from zero at low energies, as a sign of another source. Table 2 gives the net 15-240 keV rates for the two clusters for ObsIds 10271 and 20253. Both clusters in ObsId 10271 show a negative net flux, with that for cluster A being 2σ below 0.0. Investigation of the net spectra of each revealed a negative residual at 30 and 65 keV — the location of the prominent background lines. This is an indication of an under- or over-estimated livetime. The HEXTE livetime estimation is based upon a model using the Upper Level Discriminator (250 keV) and the eXtreme Upper Level Discriminator (20 MeV) rates, and on a daily timescale is accurate to $\sim$1%. Changing the livetime of cluster A off-plus by 2.1% and cluster B off-plus by 1.3% brought the net rates to 0.0 within uncertainties. ObsId 20253 data required no such change in livetime.

Since the HEXTE background has emission line features at 67 keV due to activation of the NaI(Tl) and at the lead K-lines at 74 and 85 keV due to the collimator, one must demonstrate that any claimed line features are not due to imperfect background subtraction. The brightest background line complex is at 30 keV, with a flux of 3.85×10^{-2} photons $cm^{-2}s^{-1}$. The 90% upper limit to its flux in the net Cas A spectrum is 2.18×10^{-5} photons $cm^{-2}s^{-1}$, or 0.07% of background. The 67 and 74 keV background lines have fluxes of 1.9×10^{-2} photons $cm^{-2}s^{-1}$ and 1.2×10^{-2} photons $cm^{-2}s^{-1}$, respectively. Using the percentage of background upper limit at 30 keV, we estimate the systematic sensitivity limit for the ^{44}Ti lines in this observation is 1×10^{-5} photons $cm^{-2}s^{-1}$.

Separate good time intervals were calculated for the three pointing positions of each cluster. The good time intervals required the pointing direction to be within 0.01° of the center of the Cas A remnant, its elevation above the Earth's horizon to be greater than 10°, and the time since the start of the most recent South Atlantic Anomaly passage to be greater than 20 minutes.

For each individual observation (17 each within ObsIds 10271 and 20253), the plus and minus off-source data sets were combined to form the background data set for each cluster, and the individual

source/background data for each ObsId were summed for each cluster. Finally, the ObsId 10271 and 20253 cluster A and B data were summed to form a single on-source and single off-source spectral accumulation. The resulting pulse height histogram from the two 200 ks observations contains 226 ks livetime on-source and 170 ks of real-time background. Subsequent spectral fitting was performed using these two files, as well as for the combined data in each ObsId.

The pulse height data were binned into single, 1 keV bins to 30 keV, double width bins to 89, and quadruple width bins to 100 keV. Above that energy they were combined as 100-140, 140-180, 180-220, and 220-240 keV. Three sets of data were fitted: ObsId 10271, 20253, and their sum. The data were then fitted with a power law plus two gaussian lines at the expected energies for ^{44}Ti$\rightarrow^{44}$Sc decay (67.9 and 78.4 keV). The intensities of the two lines were linked to be the same value, and line widths were considered: 1) narrow lines and 2) lines broadened by 2.5% to 1.7 and 2.0 keV respectively to account for the Cas A expansion velocity of 7500 km/s (Fesen, Becker & Goodrich 1988). The results are given in Table 3. The fit to the continuum for the two independent observations yields consistent indices and fluxes, and the best fit to the summed data is a photon index Γ=3.125$\pm$0.050 and 20-100 keV flux of 4.60$\pm$0.18$\times10^{-11}$ ergs cm^{-2}s^{-1}keV^{-1}. Fitting the ^{44}Ti line flux in the two independent observations yielded fluxes at the -0.87σ and 1.69σ level, respectively. The best fit line flux to the combined data was 1.57$\pm$2.81$\times10^{-5}$ photons cm^{-2}s^{-1}, which yielded a 90% confidence upper limit on the flux from each of the ^{44}Ti lines of 3.6$\times10^{-5}$ photons cm^{-2}s^{-1}. These values are consistent with those measured by BeppoSAX (Vink et al. 2001), and are unaffected by line widths from zero to 2 keV. The continuum was detected to 100 keV, thereby extending the maximum detected energy reported in Allen et al. (1997). The data plus best fit model for the combined data are shown in Figure 1.

Residuals to the best fit model in the case of the ObsId 10271 observation contain a large fluctuation ($\Delta\chi^2$= 8.4) in the single bin at 70 keV. Since the 2 keV width of this bin is less than the detector resolution at that energy (10 keV), the deviation is considered a statistical fluctuation. This conclusion is supported by the residuals in the ObsId 20253 data, where the residual at that energy is significantly less ($\Delta\chi^2$= 3.3).

In order to investigate the effect of a non-power law continuum, we have tried two other continuum forms: 1) a broken power law with photon index $\sim$3 up to a break energy, after which the continuum flattens (to mimic the onset of the non-thermal bremsstrahlung component as shown in Figure 1 of Ellison et al. (1999)), and 2) a high energy thermal instead of the power law to represent a steepening of the spectrum at high energies. Fitting the 20253 data, which does not have the over-subtraction of background, shows that a Γ=3 power law that breaks at 43 keV (best fit) to a Γ=2.4 power law (best fit), does not present a better fit ($\Delta\chi^2$= 0.8 for loss of 2 degrees of freedom). The 90% upper limit on the ^{44}Ti lines is reduced from 9.0 $\times10^{-5}$ photons cm^{-2}s^{-1} to 5.8 $\times10^{-5}$ photons cm^{-2}s^{-1}. Using the thermal bremsstrahlung model in place of the power law results in a worse fit ($\Delta\chi^2$= 10.1 for the same number of degrees of freedom). This model under-estimates the flux before and after the ^{44}Ti complex. The lines do become more prominent due to the dropping continuum with the upper limit rising to 1.07 $\times10^{-4}$ photons cm^{-2}s^{-1}. A steepening of the continuum, as opposed to a straight power law, is not supported by the data.

4. Discussion

The observed ^{44}Ti flux (Iyudin 1999; Vink et al. 2001) has very interesting implications for the mass of the progenitor, the supernova ejecta energy, and the question of whether the compact object left after the explosion is a neutron star or a black hole. Taking the best estimate of the mean COMPTEL and BeppoSAX flux in each of the ^{44}Ti lines to be $2.7 \pm 0.5 \times 10^{-5}$ photons/cm^2 s, we find that the ^{44}Ti yield from the Cas A supernova should be $1.5 \pm 0.3 \times 10^{-4}$ M$_\odot$, assuming an age of 317 yr for a 1997 mean date of the observations, a ^{44}Ti half-life of 59.2 ± 0.6 yr, and a distance of 3.4 kpc. This can be compared with theoretical calculations of ^{44}Ti production in core collapse supernovae.

First, we find that the ^{44}Ti yield is roughly a factor of 2 or more greater than the expected (Woosley & Weaver 1995; Nakamura et al. 2001) yields in any core collapse supernovae with ejecta energies close to $\sim 1 \times 10^{51}$ ergs, which can explain the observed properties of most (8 to 25 M$_\odot$) Type II supernovae. However, the observed yield is consistent with that expected (Woosley, Langer & Weaver 1993; Nakamura et al. 2001) from Type Ib/c supernovae of Wolf-Rayet stars with initial masses greater than 25 M$_\odot$ — implied by the optical observations (Fesen 2001; Fesen & Becker 1991; Jansen et al. 1988). In particular for a pre-collapse mass of $\sim$ 4 to 6 M$_\odot$, that would be expected (Woosley, Langer & Weaver 1993) for a WN Wolf-Rayet star that explodes before reaching the WC phase, the observed yield implies an ejecta energy of $\sim 2 \times 10^{51}$ ergs. These calculations for WN Wolf-Rayet pre-collapse stars also all predict Type Ib/c supernova explosions that leave a neutron star remnant, not a black hole.

Secondly, the predicted (Nakamura et al. 2001) ^{44}Ti/^{56}Ni ratio for the Type Ib/c supernovae of such stars is $\sim 1.7 \times 10^{-3}$, which is similar to more general predictions (Woosley & Hoffman 1991). Therefore the discrepancy between the measured ^{44}Ti yield and the estimated brightness of the historical supernova still seems to require the added effects (Nagataki et al. 1998) of an asymmmetric explosion, which has also been supported by the recent observations of (Fesen 2001).

Finally, the consistency between the observed ^{44}Ti yield and that calculated for a Type Ib/c supernova of a WN Wolf-Rayet progenitor, thus would appear to rule a black hole as the point source discovered by *Chandra* (Tananbaum 1999).

Although no pulse period has yet been detected from the Cas A compact object, comparisons of the spectral index and luminosity of the *Chandra* x-ray source with those of other x-ray pulsars suggest (Chakrabarty et al. 2001; Mereghetti, Tiengo, & Israel 2001) that it looks more like an Anomalous X-ray Pulsar/Soft Gamma-ray Repeater (AXP/SGR) than a radio pulsar. We point out that another indicator for such an association is the fact that the Cas A remnant is expanding in the warm denser phase of the interstellar medium (e.g. Higdon & Lingenfelter (1980); Hatsukade & Tsunemi (1992)), which is also the site of the bulk of the AXP/SGRs (Marsden et al. 2001). The majority of the radio pulsars, on the other hand, are observed in the hot tenuous medium where most of the core-collapse supernovae occur. Fallback disk (Alpar 2001) and push-back disk (Marsden et al. 2001) models for AXP/SGRs utilize ejecta material to form a small accretion disk around a conventional neutron star (i.e., with magnetic field of 10^{10-13} Gauss), which provides the additional torque to spin-down the neutron star rapidly and the accreted matter to generate the greater X-ray luminosity seen in AXP/SGRs. Fallback disks form within a few days from material that cannot escape the newly formed neutron star, whereas push-back disks form many years later from material decelerated by the Sedov-phase reverse shock and subsequently captured by the neutron star. We suggest Cas A is possibly in the early stages of the AXP/SGR scenario in which the push-back disk has yet to form, since the reverse shock has not reached the material in the vicinity of the neutron star. Thus, one might expect the present emission

to be indicative of a conventional cooling neutron star, as per Chakrabarty et al. (2001), and when the disk does form, the accretion will increase the luminosity to that of present-day AXP/SGRs and pulsed emission will commence.

The authors would like to thank Jacco Vink, Shigehiro Nagataki, and Anatoli Iyudin for fruitful discussions, and Harish Khandrika for data processing assistance. The authors also acknowledge the useful comments by the referee. This work was supported by NASA contract NAS5-30720.

Table 1. Log of Observations

ObsId	Dates of Observations	On-Source Livetime (ks)	Background Livetime (ks)
10271	20-28 April 1997	120.0	90.0
20253	31 March - 17 April 1996	106.2	79.8
00022	20 January 1996	12.3	10.8
10418	1-2 August 1996	2.7	2.0
30804	10 March 1998	2.9	1.5
40806	23-25 March 1999	6.8	5.8
	5 August 1999		

Table 2. Comparison of Off-Source Observations

ObsId	Cluster	Net Count Rate (c/s)
10271	A	-0.266±0.109
	B	-0.111±0.091
20253	A	-0.056±0.116
	B	-0.031±0.102

Table 3. Best Fit Cas A Spectral Parameters

Parameter	ObsId 10271	ObsId 20253	Combined
Photon Index	3.088±0.066	3.175±0.073	3.125±0.050
Flux (20-100 keV)[a]	4.76±0.25	4.41±0.25	4.60±0.18
^{44}Ti Line Flux[b]	−1.65±1.88	7.09±4.20	1.57±2.81
90% Confidence Limit[b]	≤1.85	0.72–8.99	≤3.59
χ^2/DOF	68.0/51	34.0/51	60.8/51

[a] 10^{-11} ergs cm^{-2}s^{-1}

[b] 10^{-5} photons cm^{-2}s^{-1}

REFERENCES

Ahmad, I, Bonino, G., Cini Castagnoli, G., Fischer, S.M., Kutschera, W. & Paul, M. 1998, Phys. Rev. Lett., 80, 2550

Allen, G.E. et al. 1997, ApJ, 489, L51

Alpar, A. 2001, ApJ, 544, 1245

Atoyan, A.M., Tuffs, R.J., Aharonian, F.A. & Völk, H.J. 2000, A&A, 354, 915

Arnaud, K.A., 1996, Astronomical Data Analysis Software and Systems V, eds. Jacoby G. and Barnes J., ASP Conf. Series, 101, 17

Ashworth, W.B. 1980, J. Hist. Astron., 11, 1

Baring. M.G., Ellison, D.C., Reynolds, S.P., Grenier, I.A. & Goret, P. 1999, ApJ, 513, 311

Chakrabarty, D., Pivovaroff, M.J., Hernquist, L.E., Heyl, J.S., & Narayan, R. 2001, ApJ, 548, 800

Ellison, D.C., Goret, P., Baring, M.G., Grenier, I.A. & Lagage, P.-O. 1999, in Proc. 26th ICRC, 3 468

Fesen, R.A. 2001, ApJS, 133, 161

Fesen, R.A. & Becker, R.H. 1991, ApJ, 371, 621

Fesen, R.A., Becker, R.H. & Goodrich, R.W. 1988, ApJ, 329, L89

Gaisser, T.K., Protheroe, R.J. & Stanev, T. 1998, ApJ, 492, 219

Görres, J. et al. 1998, Phys. Rev. Lett., 80, 2554

Hatsukade, I. & Tsunemi, H. 1992, in Frontiers of X-ray Astronomy, ed. Y. Tanaka & K. Koyama (Tokyo: Universal Academy Press), 387

Higdon, J. C., & Lingenfelter, R. E. 1980, ApJ, 239, 867

Iyudin, A.F. et al. 1994, A&ALetters, 284, L1

Iyudin, A.F. 1999, Nucl. Phys. A, 654, 900c

Jansen, F. et al. 1988, ApJ, 331, 949

Laming, J.M. 2001, ApJ, 563, 828

Mahoney, W.A., Ling, J.C., Wheaton, W.A., & Higdon, J.C. 1992, ApJ, 387, 314

Marsden, D., Lingenfelter, R. E., Rothschild, R. E., & Higdon, J. C., 2001, ApJ, 550, 397

Mereghetti, S., Tiengo, A., & Israel, G.L. 2001, preprint (astro-ph/0111357)

Murray, S.S., Ransom, S.M., Juda, M., Hwang, U., & Holt, S.S. 2001, preprint (astro-ph/0106516)

Nagataki, S., Hashimoto, M., Sato, K., Yamada, S., & Mochizuki, Y.S. 1998, ApJ, 492, L45

Nakamura, T., Umeda, H., Iwamoto, K., Nomoto, K., Hashimoto, M., Hix, W.R., & Thielemann, F.-K. 2001, ApJ, 555, 880

Norman, E.B. et al. 1998, Phys. Rev. C, 57, 2010

Reed, J.E., Hester, J.J., Fabian, A.C., & Winkler, P.F. 1995, ApJ, 440, 706

Rothschild, R.E. et al. 1998a, Nucl. Phys. B (Proc. Suppl.), 69/1-3, 68

Rothschild, R.E. et al. 1998b, ApJ, 496, 538

Tananbaum, H.D. 1999, IAU Circ.7246

The, L.-S. et al. 1995, ApJ, 444, 244

The, L.-S., Leising, M.D., Kurfess, J.D., Johnson, W.N., Hartmann, D.H., Gehrels, N., Grove, J.E., & Purcell, W.R. 1996, A&ASuppl. Ser., 120, 357

Timmes, F.X., Woosley, S.E., Hartmann, D.H. & Hoffman, R.D. 1996, ApJ, 464, 332

Vink, J. 1998, Nucl. Phys. B (Proc. Suppl.), 69/1-3, 62

Vink, J., Laming, J.M., Kaastra, J.S., Bleeker, J.A.M., Bloemen, H. & Oberlack, U. 2001, ApJ, 560, L79

Woosley, S.E. & Hoffman, R.D. 1991, ApJ, 368, L31

Woosley, S.E., Langer, N., & Weaver, T.A. 1993, ApJ, 411, 823

Woosley, S.E. & Weaver, T.A. 1995, ApJS, 101, 181

This preprint was prepared with the AAS LaTeX macros v5.0.

Fig. 1.— The top panel shows the counts data with 1σ error bars for the combined HEXTE observations of Cas A. Data from both HEXTE clusters have been combined and the data is binned as described in the body of this paper. The best fit model is given by the solid line. The bottom panel gives the χ value of the fit to each bin.

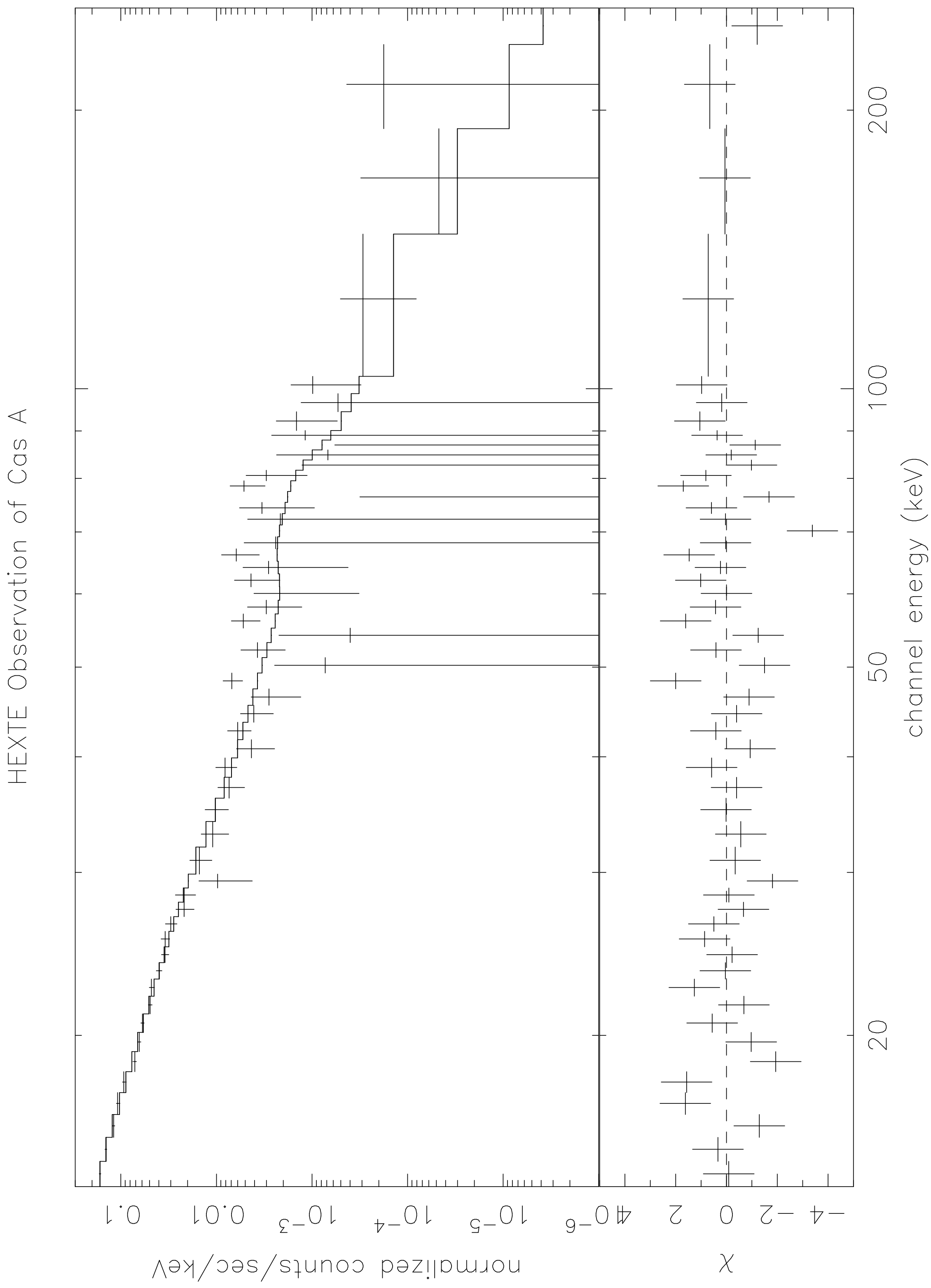
HEXTE Observation of Cas A
normalized counts/sec/keV
0.1
0.01
10^{-3}
10^{-4}
10^{-5}
10^{-6}
χ
4
2
0
−2
−4
20
50
100
200
channel energy (keV)